

11-1999

## MRI Techniques for Cardiovascular Imaging

Roderic I. Pettigrew  
*Emory University*

John N. Oshinski  
*Emory University*

George P. Chatzimavroudis  
*Cleveland State University*

W. Thomas Dixon  
*Emory University*

Follow this and additional works at: [https://engagedscholarship.csuohio.edu/encbe\\_facpub](https://engagedscholarship.csuohio.edu/encbe_facpub)

 Part of the [Bioimaging and Biomedical Optics Commons](#)

**How does access to this work benefit you? Let us know!**

### Original Citation

Pettigrew RI, Oshinski JN, Chatzimavroudis G, Dixon WT. MRI techniques for cardiovascular imaging. *Journal of Magnetic Resonance Imaging*. 1999;10:590-601.

### Repository Citation

Pettigrew, Roderic I.; Oshinski, John N.; Chatzimavroudis, George P.; and Dixon, W. Thomas, "MRI Techniques for Cardiovascular Imaging" (1999). *Chemical & Biomedical Engineering Faculty Publications*. 103.  
[https://engagedscholarship.csuohio.edu/encbe\\_facpub/103](https://engagedscholarship.csuohio.edu/encbe_facpub/103)

This Article is brought to you for free and open access by the Chemical & Biomedical Engineering Department at EngagedScholarship@CSU. It has been accepted for inclusion in Chemical & Biomedical Engineering Faculty Publications by an authorized administrator of EngagedScholarship@CSU. For more information, please contact [library.es@csuohio.edu](mailto:library.es@csuohio.edu).

# **Invited**

## **MRI Techniques for Cardiovascular Imaging**

Roderic I. Pettigrew, PhD, MD,\* John N. Oshinski, PhD, George Chatzimavroudis, PhD, and W. Thomas Dixon, PhD

THE OVERRIDING PROMISE OF cardiac MRI is that, in many diagnostic settings, it is likely to become the comprehensive test of choice. This is often referred to as a diagnostic "one-stop-shop." While other technically enhanced modalities such as gated SPECT, echocardiography with harmonic imaging, and electron beam computed tomography (EBCT) can also lay claim to this promise, the case is still most compelling for MRI. While the basic early MR techniques remain clinically viable, this evolution is becoming more compelling consequent to several technical and clinical advances that are beginning to emerge in industry, academic research laboratories, and the arena of patient care. These advances include routine black blood and cine bright blood imaging techniques that are high speed (<10 seconds per black blood image or cine slice), multislice perfusion imaging methods, and real time imaging methodologies. The application of these advances to clinical problems is also beginning to emerge in the very important area of ischemic heart disease with continued use as a problem-solving tool in some non-ischemic heart diseases. In this paper, the basic routine cardiac

imaging techniques are reviewed, and the recent technical advances that show clinical promise in functional imaging are described.

### **BASIC SEQUENCES FOR CARDIAC MRI**

The appearance and signal intensity of tissues in an MR image depend heavily on the type of imaging technique used. The two basic sequences that are most widely used are generally complementary in the appearances of the images they generate and in the type of information that can be obtained with them (Fig. 1). These are electrocardiographically (ECG) gated spin-echo (SE) and fast gradient-recalled echo imaging (1-8). This second approach is referred to by a variety of acronyms, which are different for each manufacturer of MR imaging systems. These include FFE (fast field echo), FLASH (fast low-angle shot), and GRASS (gradient-recalled acquisition in the steady state) (9-14). Variations of these basic conventional techniques have given rise to more recent ones (eg, "turbo FLASH," "turbo SE"), which can generate images in less than 1 second, as opposed to the several minutes required for earlier conventional approaches. Acquisition of the individual lines of raw image data (k-space) in groups or segments following each ECG trigger permits a complete image acquisition in 15-20 seconds. This general approach, referred to as *k-space segmentation*, can also be used to generate cine images within a breath-hold (15-17).

Spin-echo imaging is particularly useful for evaluating cardiac structure, paracardiac and intracardiac masses and thrombi, and acute and remote myocardial infarctions (10,11). The fast gradient-echo technique is excellent for evaluating regurgitant lesions, intracardiac shunts, and flow within vessels. Either technique can be used to measure right and left ventricular volumes and quantitative functional indexes, eg, biventricular ejection fractions, biventricular stroke volumes, cardiac output, radial shortening, and systolic wall thickening (2,7). However, because of greater speed of acquisition, gradient-echo-based techniques are most commonly used for functional studies.

### **Spin Echo**

The SE sequence uses two radiofrequency (RF) pulses to generate an MR signal. The first RF pulse excites the

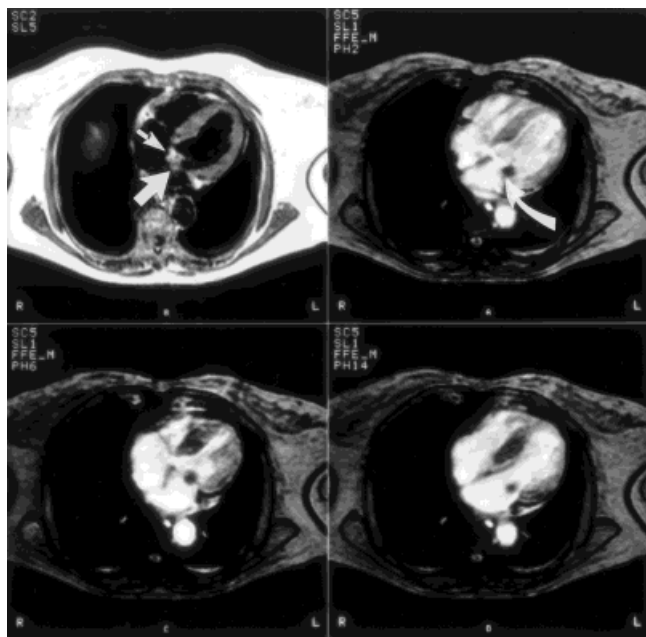


**Figure 1.** Complimentary spin-echo and gradient-echo contrast. Comparative spin-echo (upper left panel) and sequential gradient-echo images (remaining panels) of same section in a patient with a suspected left atrial myxoma. Increased signal in the left atrium (straight arrows) raises the question of slow flow vs. thrombus. Gradient-echo images at multiple phases prove spin-echo signal is due to flow but also show an apparent calcified mass as a signal void (curved arrow) attached to the posterior mitral valve leaflet. The subsequent diagnosis was fungal endocarditis. (Reproduced with permission from ref. 2.)

protons, while the second—after a brief delay—refocuses the protons to produce a coherent signal.

The basic SE sequence when conventionally applied to the heart generates an MR signal at a time that is typically 20–30 msec after the excitation pulse. A second echo can be generated and is typically at a TE of 50–90 msec. The longer echo times of the second echo emphasize greater T2 image contrast than is generated with the first echo, but at the cost of reduced signal-to-noise ratio due to greater T2 decay of the MR signal (longer decay time) (4).

SE images generated with both echoes are useful. The images obtained with the shorter echo times have a better signal-to-noise ratio and excellent contrast among epicardial fat, myocardium, and rapidly flowing blood. The absence of signal from flowing blood, called a *flow*

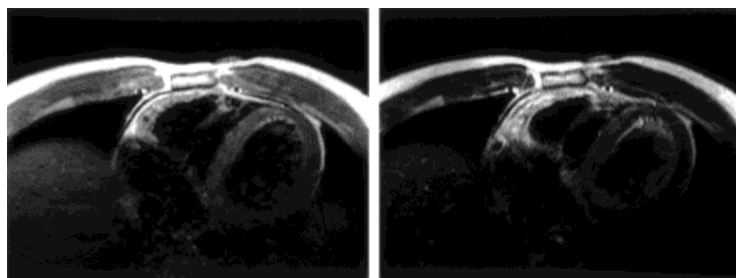
*void* or *dark blood*, is also a feature of the SE sequence (Fig. 1). This is particularly useful in providing high contrast with vascular walls, the endocardial surfaces, cardiac valves, and intracardiac septae. This flow void is due to time-of-flight effects and varies with the TE. For long TEs (ie, greater than twice the blood transit time through the slice), the blood leaves the slices before experiencing the second pulse in the SE sequence so that no signal is generated. Conversely, for short TEs the blood may remain in the section being imaged sufficiently long to experience both RF pulses and thus generate a signal (7). For typical arterial flow velocities and a typical section thickness of 10 mm, the threshold TE for a flow void is 20–25 msec. When flow rates are very slow (eg, aneurysms), a flow void may also be created by exciting the protons prior to entering the imaged section so as not to generate signal when within the imaged slice. This technique is referred to as *presaturation* (6). In general, first echo images are most useful for defining anatomic features, and visualization of vascular walls consequent to the flow void and the excellent soft tissue contrast (7).

The second echo image is most useful in detecting lesions characterized by abnormally long or short T2s, eg, acute myocardial infarction, myocardial scar, pericardial disease, cardiac masses, and thrombi (Fig. 2) (5,7). This image may also highlight slow blood flow signal seen on the first echo image as an even brighter region on the second echo image due to enhanced spin coherence for slow flow spins. This phenomenon is known as even echo rephasing (8).

### Gradient Echo

The basic gradient echo technique uses a single RF pulse to produce an echo signal. Following excitation by the RF pulse, a magnetic field gradient is used to focus the protons to produce a coherent MR signal. This signal is called a gradient echo, and the process that produces it can occur very quickly (1–10 msec) (9,10). Typically gradient echoes are obtained at TE of 2–8 msec, and this can be repeated approximately every 10–20 msec. When gated to the ECG, gradient echoes can be acquired at successive intervals of 20–40 msec throughout the cardiac cycle on almost all current systems. This permits one or more sections to be imaged at multiple phases of the cardiac cycle so that a cine display can be generated (9–14).

**Figure 2.** Dual spin-echo images of fatty infiltration in arrhythmogenic right ventricular dysplasia. First echo image (left; TE 30 msec, TR 1 R-R interval) shows increased signal in RV free wall relative to interventricular septum. Second echo image (right; TE 60 msec) is more T2-weighted, showing even greater contrast between the fatty RV and septum, similar to the fat vs muscle contrast seen in the chest wall.



Echo 1

Echo 2



Image contrast with the gradient echo technique is complementary to that obtained with the SE technique (Fig. 1). This technique produces images characterized by bright signal intensity from rapidly flowing blood. In contrast to the SE images in which rapid blood flow reduces signal, the signal intensity from flowing blood in gradient-echo images generally increases as flow velocity increases. This contrast difference is due to the different means by which the spins (protons) are refocused to generate an echo. In SE imaging, the blood must remain in the imaged section long enough for exposure to two RF pulses, whereas gradient echoes are generated after only one RF pulse. In addition, the shorter TE with gradient echoes also minimizes signal loss from spin dephasing. The signal for flowing blood can be enhanced further by a technique known as *flow compensation*. This uses additional gradient pulses, which are adjusted to eliminate motion-induced spin incoherence (9,10,14). The improved spin coherence results in less motion/flow artifact and greater signal from the following blood. This brighter blood flow feature is quite useful for imaging transvalvular flow, for the differentiation between blood flow and thrombus, for the assessment of false lumen flow in aortic dissection, and for overall improvement of image quality (10–14).

Normal intracardiac and vascular flow is bright, although variably, throughout the cardiac cycle (10–14). Flow disturbances, such as those found with regurgitant jets, ventricular or atrial septal defects, or shunts produce flame-shaped areas of signal loss that correspond to jet regions that are *intensely* turbulent (10,11). This absence of signal is due to a loss of coherent alignment of the protons within these flow patterns.

Soft tissue contrast obtained with this technique is considerably less than the contrast generated by the SE technique (Fig. 1). This is so because the gradient echo signal in static tissues (using typical cardiac MR parameters) reflects principally tissue proton density with a relatively mild T1 contribution. Consequently cardiac masses, infiltrative lesions, and non-hemorrhagic myocardial infarction may not be as readily seen with gradient echo imaging as with spin echoes (2,10).

### Turbo Spin Echo

One appealing feature of the fast gradient-echo sequence is its speed relative to SE imaging. However, a relative disadvantage is the poor soft tissue contrast. One high-speed SE-based technique (introduced over a decade ago) preserves the soft tissue contrast characteristic of routine SE images, particularly when used in combination with magnetization preparation prepulses (18,19). This basic technique, termed rapid acquisition relaxation enhancement (RARE) or more recently turbo spin echo (TSE), uses a long train of  $180^\circ$  refocusing pulses to generate multiple spin echoes after an initial  $90^\circ$  excitation pulse. Each echo in the train is phase encoded to generate a different line in k-space. Typically the echo spacing is  $\sim 10$  msec, and the effective TE is defined by the time point at which the central k-space line is obtained. This can be selected to provide T2 weighting (eg, TE<sub>eff</sub>  $\sim 60$  msec when the 6<sup>th</sup> echo occurs at  $k = 0$ ). This technique was used to rapidly read the magnetization that was initially prepared to null blood signal in Fig. 3.

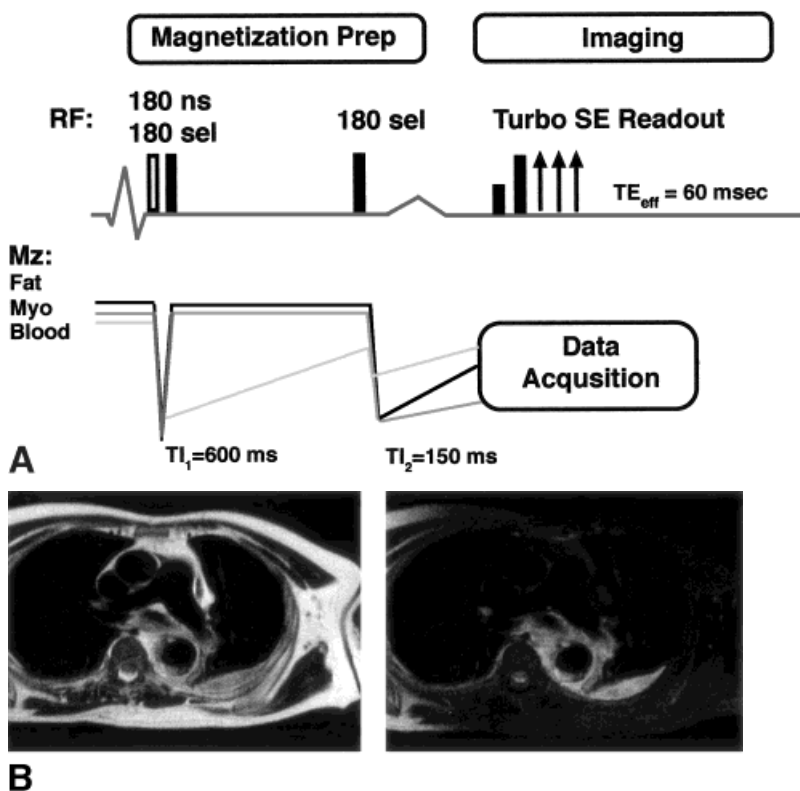


**Figure 3.** T2-weighted breath-hold black blood imaging. **A:** Schematic of technique (see text for explanation). **B:** Intramural hematoma of the descending aorta imaged with technique in A both without fat suppression (left) and with fat-suppressing TI2 inversion pulse (right). Intramural hematoma, a precursor to aortic dissection, is seen in the anteromedial aspect of the descending aorta.

### **Breath-Held Inversion Recovery for Black Blood**

This technique (Fig. 3) uses a pair of non-selective and selective  $180^\circ$  inversion pulses followed by a long inversion time (TI1) that is chosen to null the blood magnetization while the image plane tissue remains unaffected (zero net nutation). Following nulling of the blood magnetization, a second selective  $180^\circ$  inversion pulse is also applied with a short inversion time selected to null fat (STIR) and enhance contrast between long T1 and short T1 tissues. A  $90^\circ$  pulse is then applied while the heart is in relatively the same diastolic position as during the initial  $180^\circ$  pulse pair. A turbo SE readout (series of  $180^\circ$  pulses) is then used to acquire k-space lines in a segmented fashion (19). Acquiring 15 lines every second heart beat, to improve signal-to-noise ratio, permits 120 phase-encoded lines to be acquired in 16 heart beats. Thus a  $120 \times 256$  image can be generated within a breath-hold. To achieve T2 weighting, the  $\sim 6^{\text{th}}$  echo in the turbo SE train is used to produce an effective TE of 61 msec. An example of an intramural hematoma of the aorta imaged with this technique is shown in Fig. 3B. This technique has also proved very effective in imaging acute myocardial infarction, presumably highlighting the edema associated with this lesion.

## **CINE TECHNIQUES**

### **Fast Gradient Echo**

The most basic cine technique employs a flow-compensated gradient-echo sequence synchronized to the ECG (Fig. 3). In this cine technique, the gradient echo sequence is typically repeated at 20–30 msec intervals to image a single or multiple slices at a large number of consecutive points throughout the cardiac cycle. For a typical R-R interval of 800 msec, this sequence can be executed approximately 40 times so that a single heart slice could be imaged at 40 successive phases of the cardiac cycle. Alternatively, the excitation of two to three different heart slices can be interleaved such that each slice is imaged at 12–20 phases of the cardiac cycle. With this approach, in a single scan two to three slices are imaged in 128 heart beats with an image acquisition matrix of  $128 \times 128$ , generally interpolated to 256 for display. The 128 heart cycles are required since one image line of resolution for the image at each phase is acquired per heart beat. In practice, each image line may be acquired twice and averaged to improve the signal-to-noise ratio, so that the single scan time is 256 heart cycles or an average of 3–4 minutes. When multielement coil arrays are used, the signal-to-noise ratio obtained with one signal excitation may be adequate for clinical image quality so that scan time can be reduced to  $\sim 2$  minutes per scan or 3–4 minutes for six slices.

### **k-Space Segmentation: Breath-Hold Cines**

At many centers, routine cine imaging is now done during brief periods of breath-holding. Cine images of a single heart slice can be obtained within approximately 15 seconds using recent software and hardware innova-

tions (15). The basic approach uses the gradient-echo sequence, but with very short echo times of approximately 2 msec repeated at very brief intervals of approximately 10 msec. The major improvement in speed, however, results from acquiring not one but multiple lines of image resolution per heart beat for each phase in the cine sequence. By acquiring 8 lines per heart beat, the acquisition time is reduced to approximately 12 seconds, using an example of a 750 msec R-R interval (HR = 80). Since the time required to acquire the 8 image lines is approximately 80 msec, this is the approximate minimum interval at which phases of the cardiac cycle can be imaged. Consequently there is a trade-off in the temporal resolution of these cine studies so that only approximately 10 phases of the heart cycle are imaged. If greater temporal resolution is needed, the number of image resolution lines acquired per heart beat can be reduced with a proportionate increase in scan time. Image acquisition in this fashion is known as *k-space segmentation*. In this mode, k-space is acquired in multiline “segments” per heart cycle as opposed to only one data line per heart cycle (Fig. 4) (15–17).

Respiratory artifacts or degradation of image quality can be completely eliminated with this technique by simple breath-holding. Clinical experience has demonstrated improved visualization of cardiac valves, intracardiac detail, and coronaries in addition to the reduction in scan times (16,17).

### **Echoplanar Imaging: Breath-Hold Cines**

An even faster imaging technique is that of echoplanar imaging (EPI) in which single snapshot images are acquired in 40 msec or less (20–22). These images are acquired following the generation of either a conventional SE or gradient echo with subsequent rapid acquisition of all the data required to form a complete image within 30–40 msec. This ultrafast technique is achieved by rapid switching or oscillation of the spatial encoding gradients throughout the envelope of the single SE or gradient echo. In this case, all the lines of data in the image matrix are acquired within the time of a single echo, and the image is said to be formed in a single “shot.” This data acquisition method results in a decreased signal-to-noise ratio, but with a favorable trade-off in the total study time. Since the echoplanar innovation can be applied after the generation of either an SE or gradient echo, the contrast features are similar to those of T2-weighted SE images or bright blood gradient-echo sequences (22).

When implemented in these modes, dynamic studies of a single section can be obtained at a rate of from seconds (typically 16 heartbeats) to real time. While relatively few scanners, at present, are capable of EPI in the single snapshot mode as described, second-generation scanners now offer EPI in a multishot mode. This generates an image in 10–15 seconds by acquiring only a fraction of the image data per EPI sequence or “shot” and repeating this for the number of “shots” needed to fill the raw image data matrix completely (Fig. 5). This approach is less demanding mechanically and also offers better signal-to-noise ratio than the single-shot technique (23). At our institution we now routinely

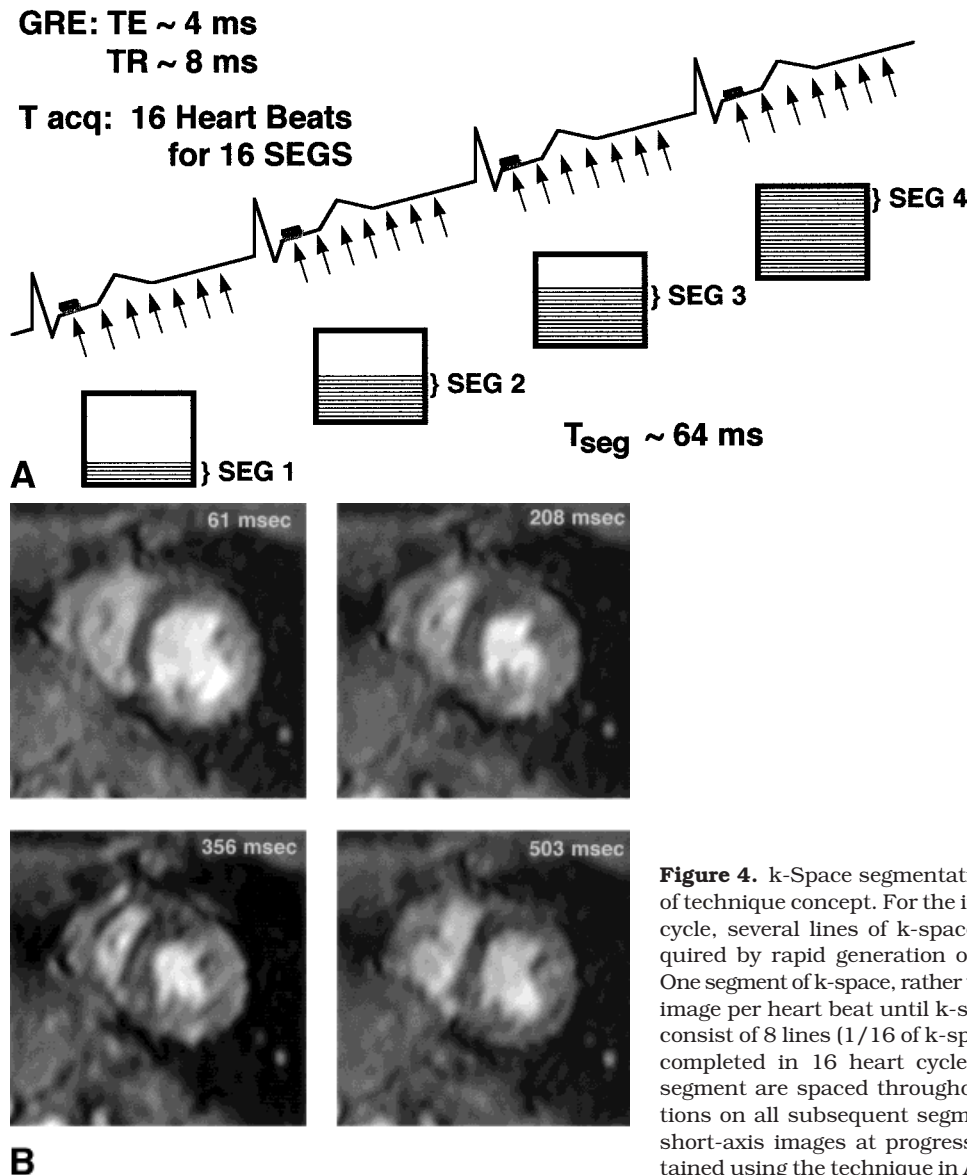


**Figure 4.** k-Space segmentation cine. **A:** Schematic illustration of technique concept. For the images at each phase of the cardiac cycle, several lines of k-space or a k-space "segment" are acquired by rapid generation of phase-encoded gradient echoes. One segment of k-space, rather than one line, is acquired per phase image per heart beat until k-space is filled. Typically, a segment consist of 8 lines (1/16 of k-space) so that the acquisition can be completed in 16 heart cycles. In practice, the lines in each segment are spaced throughout k-space with interleaved positions on all subsequent segment acquisitions. **B:** Four of eight short-axis images at progressive cycle phases from a cine obtained using the technique in A.

acquire cine images with 16 or more phases or frames per cycle in 10 seconds using a multishot EPI approach (9–12 shots with 1 shot per heart cycle). The contrast-to-noise ratio and the qualitative image quality in these images are typically superior to those of conventional cine imaging with standard gradient echoes. This is due to a combination of breath-holding, which eliminates respiratory artifact, and relatively decreased myocardial signal, resulting in enhanced blood-wall contrast that is a feature of the EPI sequence.

## FLOW QUANTIFICATION

### Basic Technique

Flow velocity quantification is based on the observation that as spins move with a velocity along an imaging magnetic field gradient, they acquire a shift in their angular position relative to stationary spins. This is called a *spin phase shift*, which is proportional to the velocity with which the spins move. This shift in the phase angle of the spins is a parameter contained within

the detected MR signal and can be readily measured (24–27). Specifically, the composite MR signal gives rise to a) the conventional image, called the modulus or magnitude image, in which the image signal intensity is simply related to the magnitude of the MR signal; and b) a phase image in which the signal intensity is proportional to the shift in spin phase relative to the stationary spins. This phase image, therefore, provides a pixel-by-pixel mapping of spin velocities, given that both the strength of the magnetic field gradient and the time during which the spins are exposed to the gradient are known. Since these features of the sequence can be explicitly prescribed, it is possible for the user to define a desired amount of spin phase shift per unit velocity and consequently determine flow rates from the phase image.

To display flow in two opposite directions, a gray scale for displaying the spin phases is chosen so that zero phase shift is medium gray. Spins that move into the scanner will typically acquire positive phase shifts of 0° to 180°. These are assigned a proportional intensity from midgray to white. Spins that move in the opposite

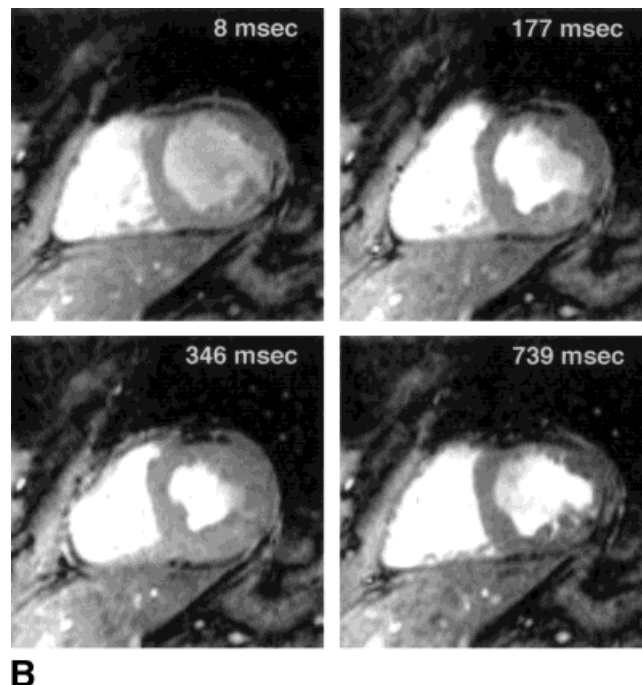
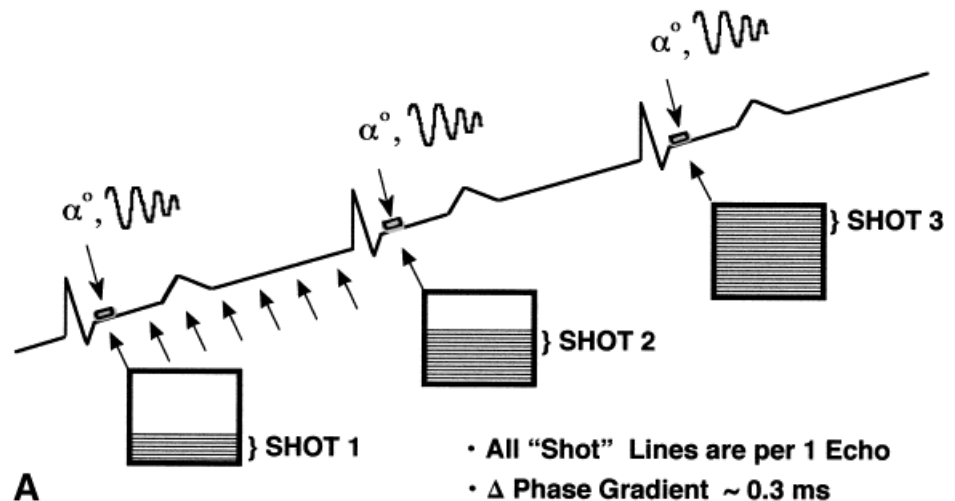


**Figure 5.** EPI cine. **A:** Schematic illustration of multi-shot technique. During each gradient echo, or "shot," multiple lines of k-space are acquired by rapid switching of the spatial encoding gradient. k-Space can be filled after only a single shot, or following multiple shots as conceptually illustrated. In practice, lines with each shot are interleaved throughout k-space. **B:** Short-axis images from a 16-phase EPI cine obtained using the technique in A.

direction will acquire negative phase shifts of  $0^\circ$  to  $-180^\circ$ . These are assigned a proportional intensity from medium gray to black. This is similar to color Doppler echocardiography, in which flow toward and away from the transducer is displayed with two different colors, red and blue.

### Valvular Regurgitation

The technique of spin-phase velocity mapping can be readily applied to quantify the severity of valvular insufficiency. The most straightforward method is to place an imaging slice perpendicular to the direction of the reverse blood flow and just proximal to the regurgitant jet. The blood velocity through that slice can be measured over the entire cross-sectional area of the vessel or flow region. Quantitative flow data is acquired throughout the cardiac cycle so that the instantaneous flow rate and the volume over any specified period of time can be calculated.

Recent studies have pointed out the importance of slice location in quantifying aortic regurgitation (28). In compliant aortic root phantom models with coronaries, and in patients, they demonstrated errors that increased as the slice location distance from the valve plane to the measurement site increased (Fig. 6). Errors of approximately 12% and 22% were measured for slice locations at the sinotubular junction and in the ascending aorta, respectively. For slice placement between the valve and the coronary ostia, the error was minimal at approximately 2%. These differences were due to the effects of aortic compliance and coronary artery filling during diastole. The predominant effect, aortic compliance, is greater with increasing distance from the valve plane. This causes underestimation of the regurgitant volume by directing flow away from the measurement slice and toward the valve during diastolic recoil. The highest accuracy is achieved by placing the slice between the aortic valve and the coronary ostia (28).



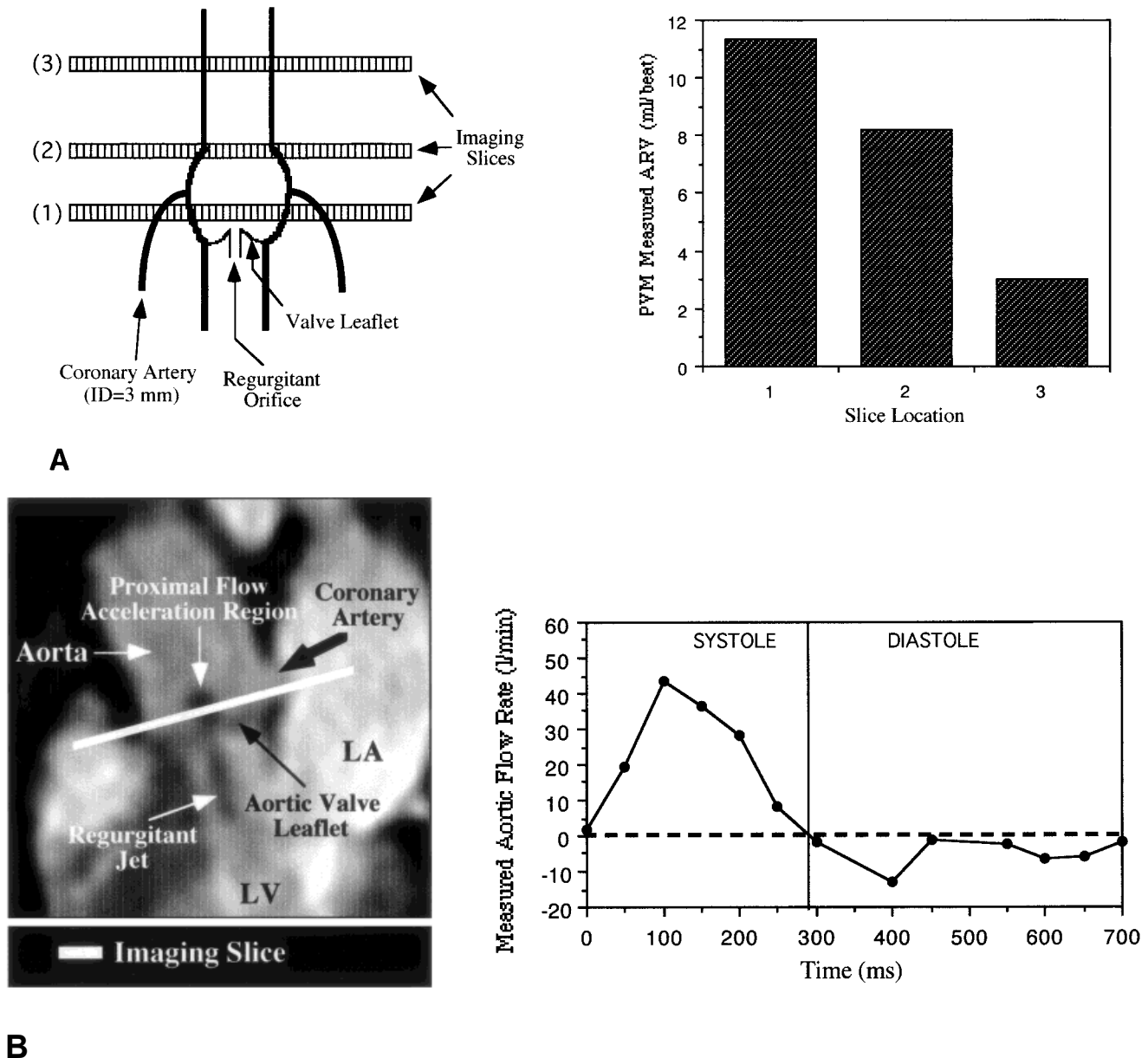


**Figure 6.** Accurate aortic regurgitation quantification. **A:** Slice location dependence of aortic regurgitation measurement accuracy. Placement of the transverse imaging/flow quantification slice at three different positions in the aorta (left) results in differing amounts of the measured regurgitant volume as shown for one representative patient (right). PVM = phase velocity mapping, ARV = aortic regurgitation volume. **B:** Optimal imaging slice placement for accurate measurement of aortic regurgitation (left) with the corresponding flow rate curve over the cardiac cycle (right). Regurgitant volume is obtained by integration of the curve over diastolic period.

The quantification of mitral regurgitation can similarly be accomplished by placing an image slice just distal to the mitral annulus. The reverse flow through this slice during systole is the regurgitant flow and can in principle be quantified from the cine phase-velocity images over the cardiac cycle. This can be complicated in practice, however, by the complex nature of the flow field in the left ventricle. In some patients there may be a significant interaction between the aortic outflow and the regurgitant flow in the vicinity of the mitral valve. In such instances, other approaches may be used. These include quantifying right and left ventricular stroke volumes by direct volumetric measurements and then

computing the stroke volume difference. This, however, requires that only one valve be regurgitant. A more recent approach, which uses a flow control volume placed around the mitral valve, has been described. This quantifies and balances the net flow from quantified flow in all three directions within this volume to determine the regurgitant flow (29).

#### Pressure Gradients

Trans-stenotic flow can be measured with sufficient signal intensity to compute velocity-encoded phase shifts when very short echo times of approximately 4 msec or



less are used. This may permit the quantification of flows through stenotic valves and stenotic vessels so that pressure gradients might in principle be approximated based on the trans-stenotic velocity change, as is currently done with Doppler echocardiography. This approach uses the Bernoulli equation in combination with the assumption that the velocity proximal to the stenosis is very much less than the peak velocity (at the vena contracta). When this condition is met, the pressure drop ( $\Delta P$ ) or gradient across the stenosis can be estimated by

$$\Delta P = KV_t^2$$

where  $V_t$  is the peak velocity in the stenosis and  $K$  is the loss coefficient, often referred to as the Bernoulli coefficient ( $\text{mmHg}\cdot\text{s}^2/\text{m}^2$ ), which is commonly taken to be 4.

However, one should note that the loss coefficient,  $K$ , is in fact a function of stenosis severity and more correctly ranges from 2.8 for a 50% stenosis to 4.9 for a 90% stenosis (27). Consequently, when  $K = 4$  is used independent of the stenosis severity,  $\Delta P$  errors on the order of 25%–40% can occur. For stenosis in the 70%–80% range,  $K = 4$  is a reasonable assumption. For other % stenoses the most accurate estimate of  $\Delta P$  is obtained by using the appropriate severity-based loss coefficient (as tabulated in ref. 27)

## MYOCARDIAL PERFUSION IMAGING

The development of high-speed MRI techniques has made it possible to assess relative perfusion of the myocardium by monitoring the first transit of a bolus of a contrast agent, eg, gadolinium-diethylene triamine pentaacetic acid (Gd-DTPA). The basic concept is as introduced several years ago. There are two fundamental goals. These are to acquire an entire image well within a heart beat and to null the myocardium in order to increase the conspicuity of the contrast agent and its passage. A nulled myocardial magnetization image is obtained pre-contrast during an acquisition window of 80–260 msec. The nulled image is produced by using a  $180^\circ$  inversion pulse before acquiring the image data, which is timed to occur when the magnetization returns from negative to zero ( $T_I \sim 300$  msec) (30). In the earliest implementations, the entire image data acquisition re-

quired a minimum of 500 msec. Hardware improvements have reduced this to 250 msec for a  $64 \times 128$  image on most systems (Fig. 7) (31).

With a nulled image being acquired well within a heart beat, the signal enhancement of the myocardium following a bolus intravenous injection of a  $T_1$  shortening agent (eg, Gd) can be monitored at heart beat intervals. The images may be visually assessed (Fig. 8) for areas of relatively delayed contrast agent arrival, and time intensity curves can be generated for any desired region of myocardium. Indexes of normal versus abnormal perfusion can be extracted from these curves for an objective assessment of relative regional perfusion (32).

## TECHNIQUE ADVANCES

### Multislice Perfusion Imaging

Despite having been demonstrated several years ago, and correlated with perfusion assessed with microspheres, perfusion imaging has not been implemented clinically, largely because the speed of the technique in the past has allowed only 1–2 slices to be imaged per heart beat. Advances in hardware and software now allow 3–5 slices to be imaged per heart beat so that 6–10 slices can be acquired with a  $2 \times (\text{R-R})$  interval temporal resolution. This permits whole-heart first-pass perfusion imaging to be qualitatively assessed and quantitative indexes of relative myocardial perfusion to be measured (32).

While not all MR systems have fast enough gradient rise times or switching speed to image multiple slices within a typical diastolic period, many new systems can acquire such images in as little as 100 msec using a hybrid turbo gradient echo (TGE) sequence ( $\text{TR} = 8$  msec) with EPI readouts to acquire 9 lines of data for each RF excitation (Fig. 8). With such short complete image acquisition times ( $\sim 100$  msec), multiple images can be acquired following magnetization preparation with the  $180^\circ$  inversion pulse (33). Trade-offs for signal and contrast to noise vs. number of slices is typically in favor of only 3 slices per heartbeat on most conventional systems. Emerging systems with high-performance gradients (40 mT/meter; 200–400  $\mu\text{sec}$  rise times) will allow an even larger number of slices to be imaged per R-R interval, so that the entire heart can be assessed for

## T1-Turbo GE

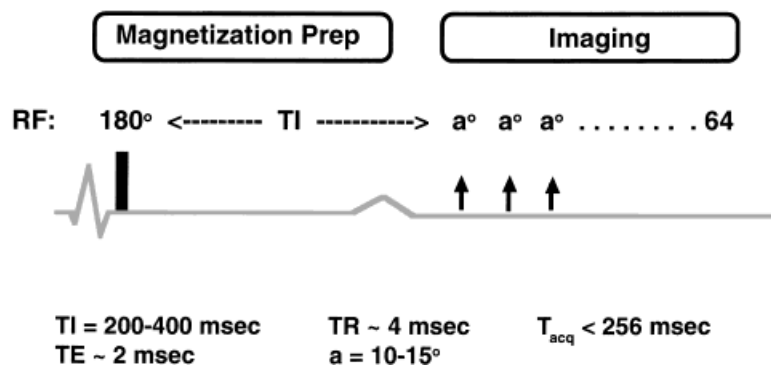


**Figure 7.** Basic method for  $T_1$ -weighted turbo gradient-recalled echo (GRE) imaging. RF = radiofrequency pulse,  $T_I$  = time of inversion, TE = time of echo, TR = repetition time,  $\alpha$  = flip angle of RF pulse,  $T_{\text{acq}}$  = image acquisition time.

- $180^\circ$  RF to null myocardium
- Turbo GE,  $TR_\alpha \sim 8\text{ms}$
- 9 line EPI Read per  $\alpha$

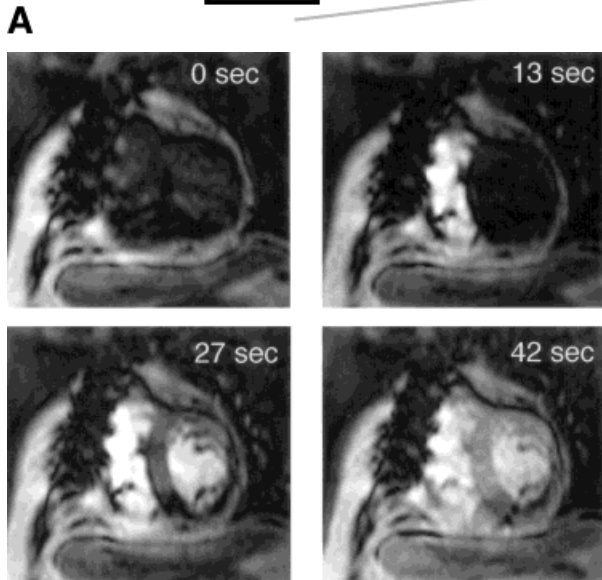
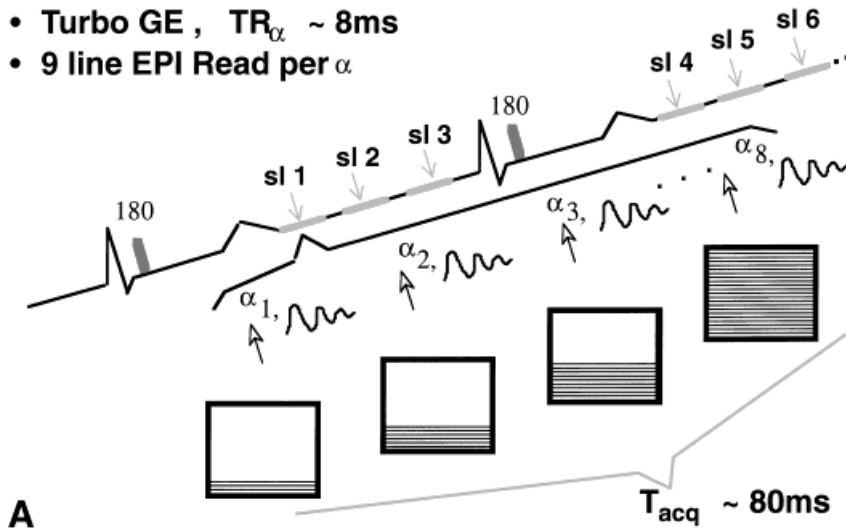


**Figure 8.** Hybrid turbo GE-EPI for multislice perfusion. **A:** Schematic illustration of technique. Following period of magnetization preparation with  $180^\circ$  inversion pulse, each of three slices is rapidly imaged during diastole. During an approximate 80 msec period, a 9-line EPI read of each of eight gradient echoes fills a 72-line k-space in eight segments. This is repeated during the next cycle to acquire three additional slices, resulting in six slices per two heart cycles. **B:** One short-axis slice from perfusion study in post CABG patient obtained with the method in A. The latter two images show relative delay in perfusion of the inferolateral segment (4:00–7:00 o'clock of the LV myocardium).

time-signal intensity changes after the Gd bolus with temporal resolution of 1–2 heart beats.

### Real Time Imaging

Cine imaging in 1–2 heart beats to real time may also be achieved by many current scanners by combining TGE with EPI readouts to acquire the entire raw data image matrix after just 8 rapid excitations (34). Each RF excitation of  $\alpha^\circ$  has a 12–16-line EPI train to acquire 100 lines of image data during an 80 msec acquisition window. This is similar to the image acquisition technique shown in Fig. 8, without the inversion pulses, and with images being sequentially acquired throughout the heart cycle at 80 msec intervals. Emerging higher slew rate gradient systems should reduce this further, and other hybrid schemes will likely emerge. One such possibility is to acquire  $\frac{1}{2}$  k-space data matrix and use symmetry arguments to fill the remainder. In so doing, 16 or more real time images could be acquired with temporal reso-

lution on the order of 70 msec over 1–2 heart beats (35). Five or more slices can be imaged with this approach during a total acquisition time of 1 minute.

Additional high-speed innovations of note are the techniques referred to as SMASH (simultaneous acquisition of spatial harmonics) and SENSE (sensitivity encoding) (35–37). These can be used to speed up acquisition times by using the spatial variation in the signal detection from each element in the phased array coils to simultaneously acquire multiple image lines of data. This is in sharp contrast to all other techniques, including EPI, in which only one line of k-space data is acquired for each phase-encode gradient step. With this approach, several lines of data are acquired per application of the phase-encoding gradient. This is therefore said to be a parallel data acquisition technique, referring to the simultaneous acquisition of multiple k-space lines. Using, for example, a four-element coil, SMASH imaging can be implemented at rates of up to four times faster to achieve real time imaging. Using a multishot

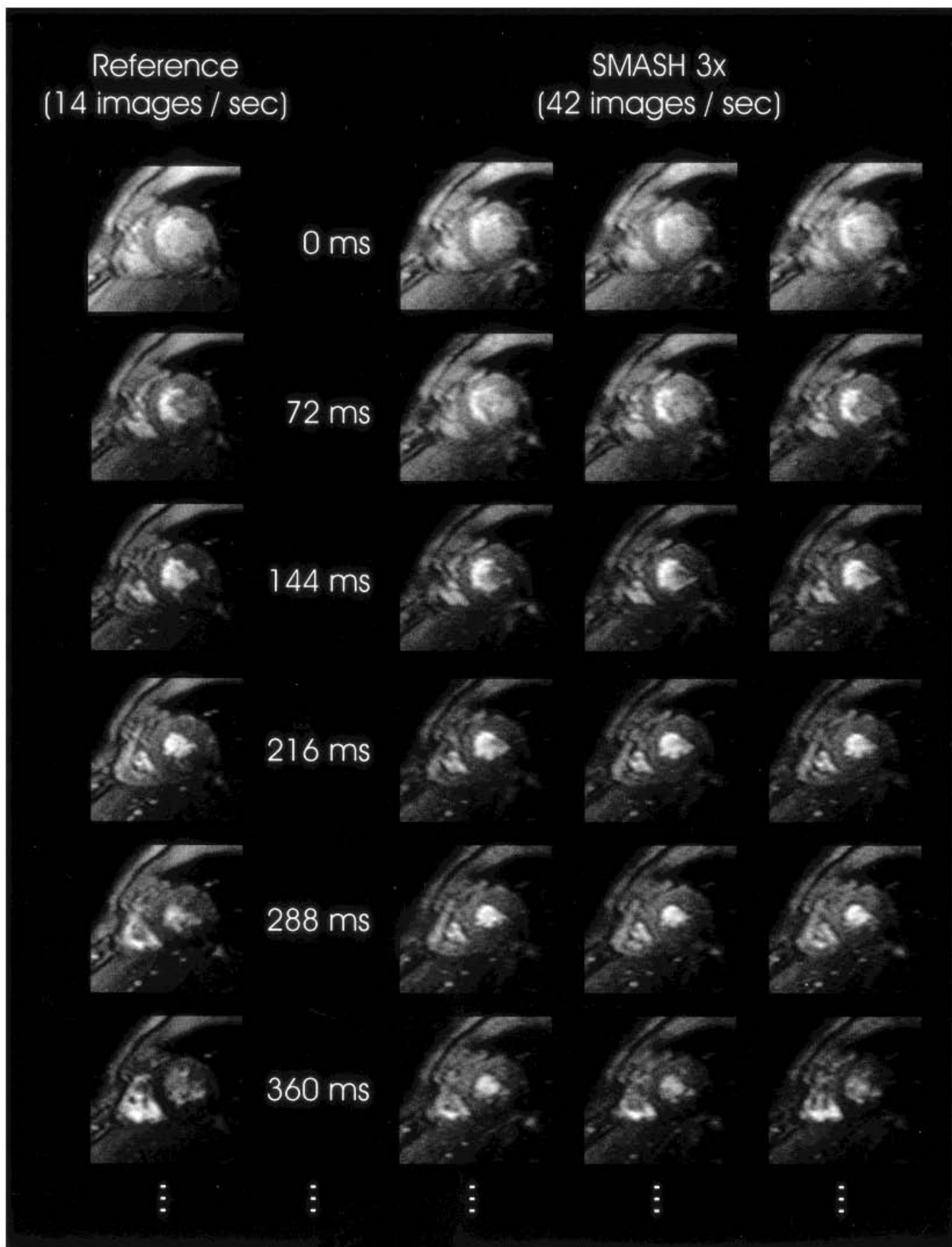


**Figure 9.** Real time SMASH images on right referenced to standard cine images on left. Acquisition time was 24 msec per image; frame rate of 42 images per second. Resolution is  $4 \times 3$  mm. (Courtesy of D. Sodickson.)

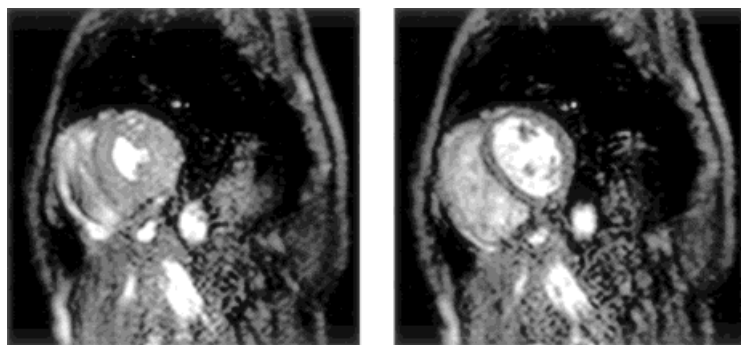


**Figure 10.** Real time imaging. End systolic (left) and end diastolic (right) images from a real time cine obtained using SENSE. Acquisition time was 27 msec per image; frame rate of 37 images per second. Resolution is 2.5 mm. (Courtesy of M. Weiger (37)).

EPI sequence with SMASH imaging, cine frame rates of up to 40 images per second have been recently demonstrated (Fig. 9). Parameters were TR 10.9 msec,  $TE_{eff}$  2.6 msec, echo spacing 1.0 msec, 7 echoes per excitation, 30° flip angle, 280 × 400 mm field of view in a 66 × 128 matrix (38). A similar approach, called SENSE, is based on measuring the sensitivity of the 3D volume seen by an array of detector coils. This technique utilizes the spatial information contained in the coil sensitivities of the multielement array for signal localization. This allows integer or fractional acceleration factors by also acquiring multiple lines of k-space data in parallel (37). These novel parallel data acquisition approaches in combination with the already high-speed sequence of multishot EPI can acquire cine images in real time while preserving clinically useful image quality (Fig. 10). One additional appeal of these techniques is that the flexibility in accelerated frame rates can be traded off for improved resolution at less accelerated, but still real time, image acquisition speeds. At present these and other techniques are at an early stage of development and clinical implementation, but they have already demonstrated significant clinical promise (38,39).

## REFERENCES

- Lanzer P, Barta C, Botvinick EH, et al. ECG-synchronized cardiac MR imaging: method and evaluation. *Radiology* 1985;155:681-686.
- Pettigrew RI. Dynamic magnetic resonance imaging in acquired heart disease: techniques and applications. *Semin Ultrasound CT Magn Reson* 1991;12:61-91.
- Hendrick RE, Raff U. Image contrast and noise. In: DD Stark, WG Bradley, eds. *Magnetic resonance imaging*, 2<sup>nd</sup> ed. Chicago: Mosby Year Book; 1992. p 109-144.
- Edelstein WA, Bottomley PA, Hart HR, Smith LS. Signal, noise, and contrast in nuclear magnetic resonance (NMR) imaging. *J Comput Assist Tomogr* 1983;7:391-401.
- von Schulthess GK, Fisher M, Crooks LE, Higgins CB. Gated MR imaging of the heart: intracardiac signals in patients and healthy subjects. *Radiology* 1985;156:125-132.
- Ehman RL, Felmlee JP. Flow artifact reduction in MRI: a review of the role of gradient moment nulling and spatial presaturation. *Magn Reson Med* 1990;14:293-307.
- Pettigrew RI. Dynamic cardiac MR imaging: techniques and applications. *Radiol Clin North Am* 1989;27:1183-1203.
- Waluch V, Bradley WG. NMR even echo rephasing in slow laminar flow. *J Comput Assist Tomogr* 1984;8:594-598.
- Van Der Meulen P, Groen JP, Bruntink T. Fast field echo Imaging: an overview and contrast calculations. *Magn Reson Imaging* 1988;6:355-368.
- Pettigrew RI. Cardiovascular imaging techniques. In: Stark, Bradley, eds. *Magnetic resonance imaging*, 2<sup>nd</sup> ed. Chicago: Mosby Yearbook; 1992. p 1605-1651.
- Utz JA, Herfkens RJ, Heinsimer JA, et al. Valvular regurgitation: dynamic MR imaging. *Radiology* 1988;168:91-94.
- Sechtem U, Pflugfelder PW, White RD, et al. Cine MR imaging: potential for the evaluation of cardiovascular function. *AJR* 1987;148:239-246.
- Frahm J, Haase A, Matthaei D. Rapid NMR imaging of dynamic processes using the FLASH technique. *Magn Reson Med* 1986;3:321-327.
- Glover GH, Pelc NJ. A rapid gated cine MRI technique. In Kressel HY, ed. *Magnetic resonance annual*. New York: Raven Press; 1988, p 299-333.
- Atkinson DJ, Edelman RR. Cineangiography of the heart in a single breath-hold with a segmented turboFLASH sequence. *Radiology* 1991;178:357-360.
- Herfkens RJ, Meyer CH, McDonnell C, Glover G, Macovski A. Clinical evaluation of breath held spiral cine MRI. *Soc Magn Reson Med Book of Abstracts*; 1992. p 108.
- Edelman RR, Manning WJ, Burstein D, Paulin S. Coronary arteries: breath-hold MR angiography. *Radiology* 1991;181:641-643.
- Henning J, Nauwerth A, Friedburg H. RARE imaging: a fast imaging method for clinical MR. *Magn Reson Med* 1986;3:823-833.
- Simonetti OP, Finn JP, White RD, Laub G, Henry DA. "Black blood" T2-weighted inversion-recovery MR imaging of the heart. *Radiology* 1996;199:49-57.
- Mansfield P. Real-time echo-planar imaging by NMR. *Br Med Bull* 1984;40:187-189.
- Chapman B, Turner R, Ordidge RJ, et al. Real-time movie imaging from a single cardiac cycle by NMR. *Magn Reson Med* 1987;5:246-254.
- Rzedzian R, Pykett I. Instant images of the human heart using a new, whole-body MR imaging system. *AJR* 1987;149:245-250.
- Davis CP, McKinnon GC, Debatin JF, Duewelle S, von Schulthess GK. Single-shot versus interleaved echo-planar MR imaging: application to visualization of cardiac valve leaflets. *J Magn Reson Imaging* 1995;5:107-112.
- Moran PR. A flow velocity zeugmatographic interlace for NMR imaging in humans. *Magn Reson Imaging* 1982;1:197-203.
- van Dijk P. Direct cardiac NMR imaging of heart wall and blood flow velocity. *J Comput Assist Tomogr* 1984;8:429-436.
- Nayler GL, Firmin DN, Longmore DB. Blood flow imaging by cine magnetic resonance. *J Comput Assist Tomogr* 1986;10:715-722.
- Oshinski JN, Parks WJ, Markou CP, et al. Improved measurement of pressure gradients in aortic coarctation by magnetic resonance imaging. *J Am Coll Cardiol* 1996;28:1818-1826.
- Chatzimavroudis GP, Walker PG, Oshinski JN, et al. Slice location dependence of aortic regurgitation measurements with MR phase velocity mapping. *Magn Reson Med* 1997;37:545-551.
- Chatzimavroudis GP, Oshinski JN, Pettigrew RI, et al. Quantification of mitral regurgitation with MR phase-velocity mapping using a control volume method. *J Magn Reson Imaging* 1998;8:577-582.
- Atkinson DJ, Burstein D, Edelmann RR. First-pass cardiac perfusion: evaluation with ultrafast MR imaging. *Radiology* 1990;174:757-762.
- Pettigrew RI, Oshinski J, Dixon WT. Magnetic resonance imaging techniques for assessing myocardial perfusion. In: C Higgins, J Ingwall, G Pohost, eds. *Current and future applications of magnetic resonance in cardiovascular disease*. Mt. Kisco, NY: Futura; 1998.



32. Wilke N, Jerosch-Herold M, Wang Y, et al. Myocardial perfusion reserve: assessment with multisection, quantitative, first-pass MR imaging. *Radiology* 1997;204:373–384.
33. Ding S, Wolff SD, Epstein FH. Improved coverage in dynamic contrast-enhanced cardiac MRI using interleaved gradient-echo EPI. *Magn Reson Med* 1998;39:514.
34. Ridgway JP, Kassner A, Beacock DJ, Sivananthan UM. Fast left ventricular volume measurement using a multiple-slice 'real-time' acquisition: a pilot study. In: *Proceedings of the International Society for Magnetic Resonance in Medicine Seventh Scientific Meeting and Exhibition*, Philadelphia, May 22–28, 1999.
35. Sodickson DK, Stuber M, Botnar RM, Kissinger KV, Manning WJ. SMASH real-time cardiac MR imaging at echocardiographic frame rates. In: *Proceedings of the International Society for Magnetic Resonance in Medicine Seventh Scientific Meeting and Exhibition*, Philadelphia, May 22–28, 1999.
36. Sodickson DK, Manning WJ. Simultaneous acquisition of spatial harmonics (SMASH). *Magn Reson Med* 1997;38:591.
37. Weiger M, Pruessmann KP, Boesiger P. Cardiac real-time imaging using SENSE. *Magn Reson Med* (in press).
38. Debbins JP, Riederer SJ, Rossman PJ, et al. Cardiac magnetic resonance fluoroscopy. *Magn Reson Med* 1996;36:588–595.
39. Kerr AB, Pauly JM, Hu BS, et al. Real-time interactive MRI on a conventional scanner. *Magn Reson Med* 1997;38:355–367.